Multiple Alignment Modes for Nematic Liquid Crystals Doped with Alkylthiol-Capped Gold Nanoparticles

Hao Qi and Torsten Hegmann*

Department of Chemistry, University of Manitoba, 144 Dysart Road, Winnipeg, Manitoba, R3T 2N2 Canada

ABSTRACT The ability of alkylthiol capped gold nanoparticles (Au NPs) to tune, alter, and reverse the alignment of nematic liquid crystals (LCs) has been investigated in detail. Adjusting the concentration of the suspended Au NPs in the nematic LC host, optimizing the sample preparation protocol, or providing different sample substrates (untreated glass slides, rubbed polyimide-coated LC test cell, or ITO-coated glass slides) results in several LC alignment scenarios (modes) including vertical alignment, planar alignment, and a thermally controlled alignment switch between these two alignment modes. The latter thermal switch between planar and homeotropic alignment was observed particularly for lower concentrations (i.e., around 1 to 2 wt %) of suspended NPs in the size regime of 1.5−2 nm and was found to be concentration-dependent and thermally reversible. Different scenarios are discussed that could explain these induced alignment modes. In one scenario, the NP-induced alignment is related to the temperature-dependent change of the order parameter, *S*, of the nematic phase (ordering in the bulk). In the second scenario, a change of the ordering of the nematic molecules around the NPs that reside at the interfaces is described. We also started to test spin coating as an alternative way of preparing nematic thin films with well-separated Au NPs on the substrate and found this to be a possible method for manufacturing of future NP-doped LC devices, as this method produced evenly distributed NPs on glass substrates. Together the presented findings continue to pave the way for LC display-related applications of Au NP-doped nematic LCs and provide insights for N-LC sensor applications.

KEYWORDS: liquid crystals • nematic • nanoparticle • gold • liquid crystal alignment • order parameter • liquid crystal displays • liquid crystal sensors

INTRODUCTION

The use of liquid crystals (LCs) in many high-tech devices, such as light shutters and modulators (1−4), sensors (5−10), and of course liquid crystal displays (LCDs) (11−13), is intimately connected to the necessity to macroscopically align liquid crystal molecules along a preferred direction (energetically favorable direction or easy axis) (14).

Many materials and methods have been developed over the past decades, yet one of the early methods for LC alignment, the use of rubbed polymer alignment layers, is still the method of choice for the manufacturing of small and large panel LCDs (14). However, the easy and cheap method providing stable alignment of nematic and smectic LCs for different display modes also has numerous disadvantages, such as polymer debris resulting from the rubbing with a velvet cloth (using rubbing machines) and inhomogeneous, site-dependent contrast ratios in the final display, which can only be avoided by careful monitoring of the manufacturing conditions in clean rooms (15). Because of their high thermal stability and mechanical strength, polyimides are most commonly used as rubbed polymer alignment materials, and significant research efforts have been geared toward modulating the chemical structure of polyimides. Chemical modification and mixing of different polyimides now allow for improved planar alignment (i.e., the long molecular axis of rod-like nematic LCs aligns parallel to the surface) (16−19), homeotropic (vertical) alignment of rod-like LCs, commonly without rubbing (i.e., the short molecular axis aligns parallel to the surface) (20−22), or enable tuning of the LC alignment between planar and vertical. (i.e., tuning the pretilt angle of the LC molecules) (24−27).

An alternative method to achieve LC alignment is photoalignment (a noncontact technique) using molecules, usually tethered to the substrate, containing structural features that can be reversibly isomerized by irradiation with light of different wavelengths resulting in a change of the overall molecular shape. One of the most investigated class of materials for photoalignment of LCs are azobenzenes (28−38), but low thermal stability and noncontrollable, random cis−trans relaxations severely limit implementation of azobenzene-derived photoalignment layers for display applications. Other compounds tethered to surfaces allowing for photoalignment of LCs include cinnamoyl-based chromophores (16, 39−46), the spyropyran-merocyanine isomer couple (47−51), and coumarines (52−55). Other polymers such polystyrene (56) and oligosiloxanes (57−60) with hydrocarbon linkers to aromatic cores, such as naphthalene or pyridine, were also found very capable of imposing alignment onto nematic LCs, some requiring rubbing, others not.

* To whom correspondence should be addressed. E-mail: hegmannt@cc.umanitoba.ca.

Received for review April 27, 2009 and accepted June 30, 2009

DOI: 10.1021/am9002815

More recently, nanoscale manufacturing and self-assembly techniques have also found entrance into the area of LC alignment. One prominent technique, extensively utilized by Abbott et al. (10, 61−64), makes use of alkylthiol self-assembled monolayers (SAMs) either on thin gold films sputtered on glass or gold islands (i.e., nanoparticles) immobilized on surfaces via electron beam evaporation, which, depending on the chain length, combination of chain lengths, and functionalization, can induce multiple alignment scenarios in nematic LCs (65, 66). Another technique employs either glancing angle ion-beam deposition (67, 68), as well as ion beam (21, 69−78) or plasma bombardment (79−87) of thin polymer, SiN_x, diamond-like carbon, or other thin films deposited on substrates. Of these techniques, the glancing angle ion beam bombardment of diamond-like carbon is already used for the manufacturing of smaller LCD panels by IBM (78, 88).

Concurrently, recent years have also seen a tremendous increase in the number of reports describing the use of nanoparticles (NPs) dispersed in LCs (NP-doped LCs or LC/NP composites) to yield macroscopic alignment of LCs, and in some instances, the alignment altered or induced by the NPs comes jointly with the manipulation of other LC properties or LCD-relevant characteristics, such as threshold voltage, pretilt, dielectric behavior, or contrast ratio (25, 89−98). The most prominent among these nanoparticulate systems are oligomeric silsesquioxanes NPs with size from 0.7−30 Å inducing vertical alignment (25, 89), carbon nanotubes (99−101), fullerenes (102), and gold nanoparticles (Au NPs) developed by our group (91, 93, 95−98).

LC/Au NP composites represent a combination of the properties of LCs with the size-dependent characteristics of Au NPs with mutual benefits for both components. On the one hand, Au NP properties can be tuned by surrounding them with LCs introducing changes of the localized surface plasmon resonances (61), and more importantly, liquid crystal are unique candidates to manipulate Au NP assembly (103, 104), which is important for exploring the spatial arrangement of Au NPs, as well as their related fundamental electronic and optical properties for constructing novel nanoscale devices (105, 106). On the other hand, the properties of liquid crystals can also be affected by the Au NPs, such as electro-optic properties (107) and alignment of LC molecules used in display applications (93). These mutual benefits are most likely not limited to Au NPs; NPs with other core materials (metal, metal oxides, etc.) should work as well.

Earlier work by our group described an LC alignment phenomenon for nematic LCs doped with Au NPs. In mixtures of pure nematics containing 5 wt % of alkyl thiolate-capped Au NPs, the formation of quasi-periodic, birefringent stripe patterns separated by areas of homeotropic alignment of the LC molecules was observed, which appeared, in part, remarkably similar to fingerprint or cholesteric finger textures, although neither the LC hosts nor the NPs were chiral (95). More detailed studies to understand the origin of these textural and alignment effects (97) provided insight that this

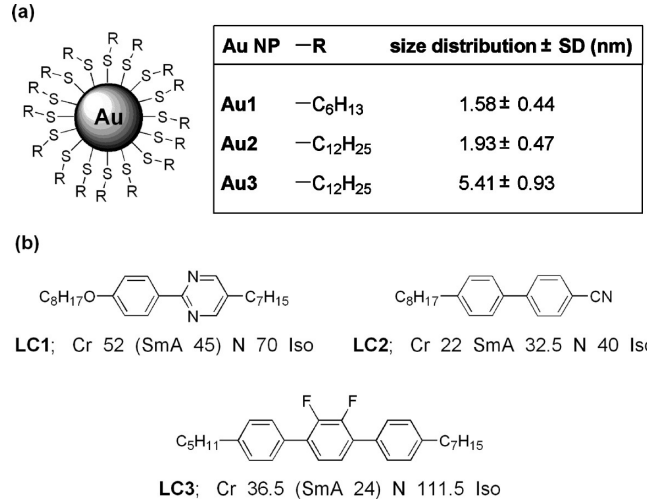

FIGURE 1. (a) Schematic of alkyl thiolate capped Au1−Au3 NPs including size distributions (SD = standard deviation) obtained by transmission electron microscopy, TEM (TEM image analysis of all NPs in each image was performed with the following software: Scion Image Beta 4 (Scion Corp.) or Image J), (b) chemical structure and LC mesomorphism including phase transition temperatures (°C) of LC1−LC3 (abbreviations Cr = crystalline solid state, SmA = smectic-A phase, *N* = nematic phase, Iso = isotropic liquid phase).

phenomenon can be used as a way to control the alignment of LC molecules using functionalized Au NPs, which is a requirement for all LC display application but particularly interesting for vertical alignment (VA) mode displays. In due course, we also established an unprecedented dual alignment and electro-optic mode in the same system using planar ITO cells with rubbed polyimide alignment layers. In this mode, LCs with a positive dielectric anisotropy can be initially homeotropically aligned, then tuned to change to planar alignment, and most astonishingly, switched between optical ON and OFF states by applying an electric field (93). In addition to Au NPs, we also demonstrated this phenomenon for Ag NPs and CdTe quantum dots (98), which taught us that this is likely a general phenomenon given that the NPs can be reasonably well dispersed in the nematic LC host, that the NPs fall within a certain size regime, and that they are protected with LC compatible, not necessarily LC capping agents (96).

In this paper, we will describe several ways to control the alignment of nematic LCs using Au NPs in more detail. Critical aspects of the alignment induced by Au NPs in different nematic LCs such as NP concentration, NP size, and length of the carbon chain of the alkyl thiolate capping the NPs were investigated with a particular focus on different sample preparation techniques. To realize this, we used three different Au NPs varying first the length of the alkyl thiolate (**Au1** with C_6H_{13} vs **Au2** with $C_{12}H_{25}$) accompanied by only a small change in size, and then the size (~2 nm for **Au2** vs 5.4 nm for **Au3**) in three structurally different LC hosts **LC1**−**LC3** (Figure 1). We first examined induced alignment effects using a lower concentration of initially finely dispersed Au NPs in nematic suspensions, since 5 wt % suspensions, as described above, result in homeotropic (vertical) alignment immediately at the transition from the isotropic liquid to the nematic phase ($T_{Iso\text{-}N}$). We then pro-

ceeded to study if preloading the cells with the Au NPs (i.e., fixation of the NPs at the LC test cell polyimide alignment layers) followed by filling the cells with the nematic LCs reduced the number of birefringent stripe defects. Finally, we also extended these studies to nematic LCs with negative dielectric anisotropy (**LC3**), which are used in VA mode LCDs, and made initial inroads toward spin-coating of LC/Au NP composites as a means of manufacturing displays with NP induced alignment and enhanced electro-optic characteristics.

EXPERIMENTAL SECTION

Three different Au NPs (**Au1**−**Au3**) and three different LC hosts (**LC1**−**LC3**) were used. A description of the synthesis and the characterization of **Au1**−**Au3** can be found in earlier papers (for **Au1** and **Au2** see ref 108, for **Au3** see ref 98). The three used LCs are commercially available: **LC1** was purchased from Synthon Chemicals GmbH, **LC2** from Merck KGaA, and **LC3** from Kingston Chemicals, Ltd. The composition and size of the Au NPs and the structure and LC phase behavior of **LC1**−**LC3** are shown in Figure 1. Transparent, conductive indium tin oxide (ITO) coated glass slides were purchased from Delta Technologies, Ltd. The LC test cells used were planar 5.0 μm cells with antiparallel polyimide alignment layers with low pretilt (Displaytech Inc., purchased from Linkam Scientific Instruments). All particles were stored as dry solids under a protective atmosphere of dry N_2 in the dark, and can be repeatedly dispersed in and isolated from selected organic solvents without change in size (no aggregation or ripening). All glass vials and Teflon-coated spatulas were rinsed with aqua regia prior to all mixture preparations.

Transmission electron microscopy was performed on a Jeol ultrahigh resolution FEG-T/STEM operating at an accelerating voltage of 200 kV. A 10 μL drop of the cluster solution was drop-cast on a carbon-coated copper grid (400-mesh) and dried for 1 h. Polarized optical microscopy (POM) was performed using an Olympus BX51-P polarizing microscope in conjunction with a Linkam LS350 heating/cooling stage. To apply electric fields an LCAS I automated liquid crystal analyzer (LC Vision) was used. Spin-coating of LC/Au NP suspensions on glass substrates was performed using a Laurell Technologies Corp. WS-400B-6NPP spin coater. AFM investigations were done on a Multi-Mode SPM (Digital Instruments) in tapping mode.

The alignment experiments were pursued using precleaned standard 1 × 4 in. microscopy glass slides plus coverslips (Fisher Scientific), homemade cells using transparent ITO-coated glass slides, or commercially available planar LC cells with parallel or antiparallel rubbed polyimide alignment layers. The reproducibility of the alignment effects and EO measurements was checked on several cells for each composition. All Au NPs nematic suspensions were prepared by combining solutions of the LC and the NP in a common, pure, and dry solvent (e.g., ethyl acetate). The resulting solutions were stirred (agitated) for at least 10 min, and thereafter, the solvent was evaporated under a steady stream of dry N_2 over open glass vials, and all mixtures were then dried in vacuum for 24 h. Prior investigating these suspensions between untreated microscopy glass slides and prior to filling LC test cells by capillary forces with the LC in the isotropic liquid phase, all mixtures were heated just below the isotropic−nematic phase transition ($T_{Iso/N}$) and continuously mixed again. Preloading of the cells with Au NPs was performed by filling the cells with a few drops of the Au NPs dispersed in *n*-hexane and drying the cell (mild heat, i.e. just above the bp of the solvent) prior to filling it with the nematic LC containing the remaining amount of the Au NPs dispersed in the nematic LC. In probe experiments, we firmly established that *n*-hexane had no effect on the quality and homogeneity of the induced planar alignment of the pure nematic LC (see Supporting Information).

RESULTS AND DISCUSSION

Alignment Studies Using Au NP-Nematic Suspensions. The first part of this study was dedicated to help understand if the induced vertical alignment of nematic LCs by Au NPs is concentration dependent. Previous work had shown that higher concentrations of alkyl thiolate-capped Au NPs in nematic suspensions (around 5 wt %) are well capable of inducing vertical alignment of nematic LCs (93) but also tend to favor the formation of NP aggregates (96). We then anticipated that lower concentrations of NPs, at a certain threshold, would produce *Schlieren* textures commonly observed for pure nematic LCs or textures displaying a coexistence of birefringent stripe domains surrounded by vertically aligned domains and planar *Schlieren* texture domains. For example, with careful sample preparation and slow cooling, **LC1** doped with alkyl thiolate-capped Au NPs (with 1−2 nm core diameters) often produces homeotropic aligned LCs between untreated microscopy glass slides without noticeable NP aggregation (95). Partially homeotropic aligned nematic LCs via NP doping have also been demonstrated by Cabuil et al. (109) and Bezrodna and co-workers (110), although no discussions of this effect was disclosed. We trust that the qualitatively better and more homogeneous vertical alignment observed for the Au NPs is the result of the better solubility (enhanced compatibility) of Au NPs in comparison to the bare maghemite (109) or the octadecylbenzyldimethyl-ammonium chloride modified organoclay NPs used by the other groups (110). Cabuil et al. in their report (109) also described a reversed gathering or dispersing of NPs at the Iso-N transition temperature, which is likely related to the different solubility of NPs in the nematic 5CB host in the isotropic or LC phase, respectively. We also observed the formation of smaller, micrometer-sized NP aggregates by observing the sample with uncrossed polarizers in our previous studies (93) using higher Au NP concentrations when cooling well-dispersed LC/Au-NP suspensions from the isotropic to the N phase. Hence, we predict that for a certain size and concentration regime the Au NP solubility will also change in the N phase itself depending on temperature. Recent molecular dynamics simulations of a model system (NP and nematogen with equal NP diameter and length of the nematic spherocylinder) by Smith and Glaser confirm this prediction (111). As order and hence order parameter *S* of a nematic phase increase with decreasing temperature, the solubility of NPs is certainly affected at a specific temperature (solubility threshold). Keeping this thought in mind, we examined several nematic LC/Au NP suspensions with 1 or 2 wt % **Au2** NPs in **LC1**, which we initially thought of showing pure nematic *Schlieren* textures and found what we termed a *thermal alignment switch* phenomenon. As shown in Figure 2a−d, as the temperature decreases, the LC texture changes from a typical nematic *Schlieren* texture to vertical alignment with very few birefringent stripe defects. Observing the texture in Figure 2d with parallel polarizers (Figure 2e) shows

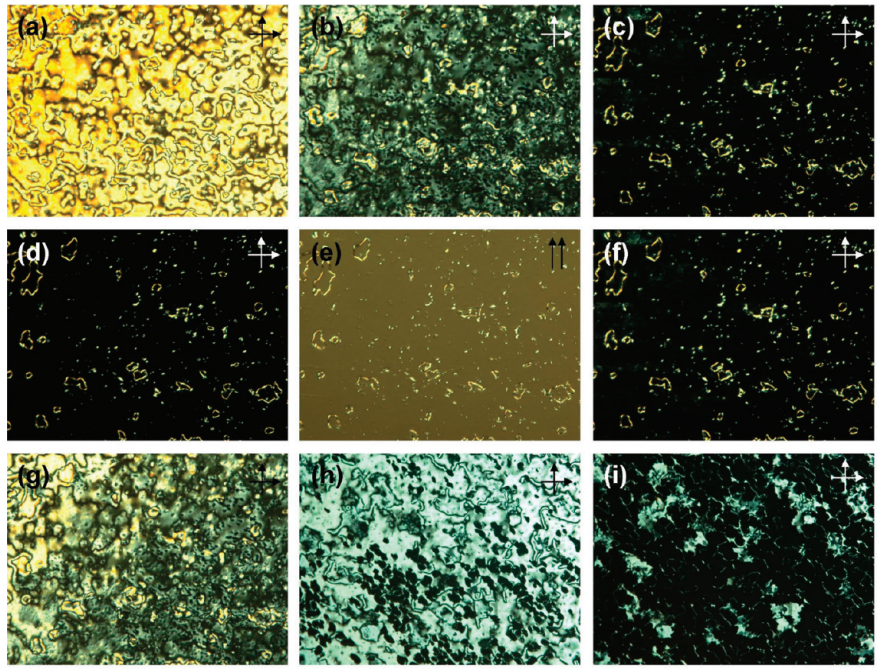

FIGURE 2. POM photographs: LC1 with 2 wt % Au2 from cooling at (a) 64.0, (b) 61.0, (c) 58.9, and (d) 56.0 °C with crossed polarizers and at (e) 56.0 °C with parallel polarizers (lower light intensity). The same area observed on heating at (f) 59.0 and (g) 62.0 °C. LC1 with 1 wt % Au2 from cooling at (h) 49.8 and (i) 48.5 °C (white or black arrows indicate polarizer and analyzer position).

no noticeable NP aggregation for this sample at the micrometer scale and only the previously discussed birefringent stripe defects. This thermal alignment switch from parallel alignment (*Schlieren* texture, optical ON state) to vertical alignment (optical OFF state) is surely related to the change of solubility of the NPs in the LC host. At higher temperature, the NPs are dispersed in the LC matrix, and the LC molecules interacting with the glass surface dominate the alignment. At lower temperature, the increased order (i.e., order parameter) of nematic LC molecules (phase), expels some amount of the NPs to the glass-LC interface, where the NPs induce or control the alignment of the nematic LC molecules similar to mixed thiol SAMs on planar Au surfaces (64). Another possibility, that we cannot exclude with the data available, is a change in the temperature-dependent ordering of the LC molecules near NPs that are permanently localized near the LC/alignment layer interface. If one or the other mechanism is active, this thermal alignment switch should be reversible.

As shown in Figure 2f and g, by heating the sample starting at the low-temperature vertical alignment, planar alignment with a *Schlieren* texture reoccurs at practically the same temperature. We also found that the temperature of this thermal alignment switch is concentration dependent. Lowering the NP concentration from 2 to 1 wt % resulted in a lower alignment switch temperature of about 10 °C as shown in Figure 2h and i.

This phenomenon shows that the NPs residing at the interface and inducing vertical alignment of nematic LCs is dynamic rather than static, and means that the NPs either can be located at the interface or be dissolved in the bulk of nematic LCs (based on the first mechanism) or that the ordering of the LCs around the NPs changes drastically enough (based on the second mechanism) simply by tuning the temperature. Hence, the established picture of better NP solubility in the isotropic liquid phase and much lower solubility at the phase transition to the nematic phase has to be extended to the solubility change or adjustment within the nematic phase itself. A movie clip of this thermal alignment switching effect can be viewed in the Supporting Information.

We also observed this thermal alignment switch phenomenon in ITO LC test cells with rubbed polyimide alignment layers. Due to the preferential planar anchoring of the used nematic LCs on the rubbed polyimide alignment layers, we normally could only observe either homogeneous vertical alignment at higher Au NP concentration (~5 wt %) or planar alignment at lower NP concentrations. However, the thermal alignment switch was here observed for **LC1** doped with 10 wt % of the larger **Au3** NPs. Keeping in mind that we used smaller size Au NPs in all experiments discussed above (around 1−2 nm), this mixture with **Au3**, because of the larger size of the **Au3** NPs (5.4 nm), even at 10 wt % only contains about 10% of the total number of Au NPs in comparison to the 5 wt % **Au2** in **LC1** mixture. In other words, 10 wt % **Au3** in a nematic suspension equal 0.5 wt % of **Au2** in the same LC, although we expect that the different size will also play a role in controlling the LC alignment. While the nematic phase of **LC1** containing 10 wt % **Au3** shows vertical alignment over the entire nematic phase range between untreated microscopy glass slides, the same mixtures shows the thermal alignment switch in the LC test cell as shown in Figure 3a and b. The same phenomenon has also been observed with a more polar nematic LC host **LC2** (8CB) doped, for example, with 5 wt % of the smaller Au NPs **Au2** (Figure 3c and d), which shows that this effect is likely universal to these NP nematic LC combinations given excellent control over cooling rates and ideal

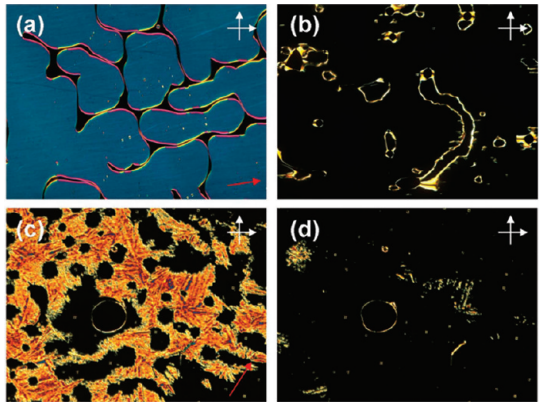

FIGURE 3. POM photographs of thermal alignment switch in planar, rubbed polyimide coated ITO cells: LC1 with 10 wt % Au3 from cooling at (a) 56.0 °C with some isotropic domains still present and (b) 48.0 °C; LC2 with 5 wt % Au2 from cooling at (c) 35.5 °C showing a coexistence of planar and homeotropic domains and (d) 33.7 °C (white arrows indicate polarizer and analyzer position).

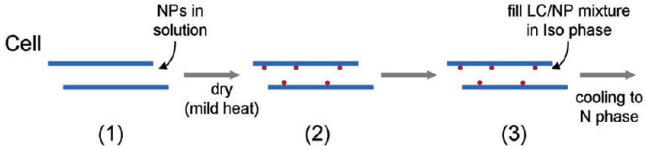

FIGURE 4. Procedure for preparing Au NP preloaded LC test cells.

sample preparation conditions. Not surprisingly, the thermal alignment switch was observed commonly for lower concentrations of the smaller **Au1** and **Au2** NPs (~1−2 wt %) and for higher concentrations of the larger **Au3** NPs (around 10 wt %) in **LC1** and **LC2**. While a potential application of this thermal alignment switch phenomenon has not yet been demonstrated, the design of LC biosensors (e.g., for sensing spherical proteins or other biomolecules using sandwiched LC films) (10) could benefit from this reversible and drastic change in light transmittance as a result of the bulk alignment change from vertical to planar at relatively low NP concentrations and maybe also in combination with binding of biomolecules to Au NPs (112, 113).

Preloading Cells with Au NPs. The second part of this study now focuses on sample preparation effects. We want to show that the alignment of nematic LCs can not only be tuned by dispersing alkyl thiolate-capped Au NPs in nematic LCs at different concentrations but also that different ways of preparing the final sandwiched thin film sample can have a tremendous effect. The questions we asked were as follows: (1) Will immobilizing Au NPs on the alignment layers improve the quality of the alignment? (2) Is the thermal alignment switch also observed with this sample treatment? (3) Could spin-coating of nematic LC/Au NP suspensions be used as a way to manufacture NP-doped LC mixtures that do not require alignment layers?

Let us take **LC1** doped with 10 wt % **Au3** as an example. The thermal alignment switch of this mixture was discussed in the section above. Now, after we enriched the NP concentration at the glass/LC interface or alignment layer/LC interface, we only observed vertical alignment and no sudden change from planar to vertical at a given temperature. The process that allows maintaining a total 10 wt % of

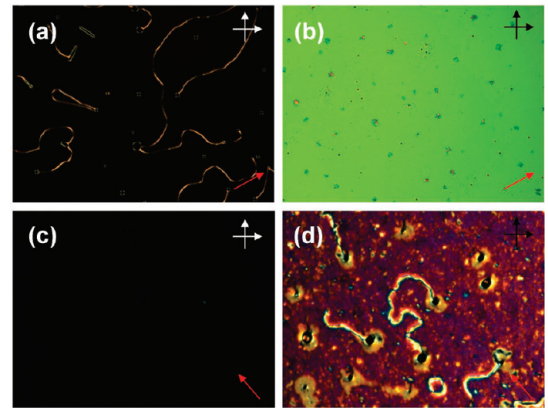

FIGURE 5. POM photographs of cells using the method of preloading a portion of the NPs: (a) LC1 with 10 wt % Au3, as-prepared cell on cooling at 60.2 °C and (b) on cooling from isotropic liquid phase to the N phase with a 5 V dc electric field to reverse the alignment to a planar aligned texture at 59.7 °C. (c) LC2 with 5 wt % Au2, as-prepared cell on cooling at 33.5 °C and (d) on cooling from the isotropic liquid phase to the N phase with a 5 V dc electric field to reverse the alignment to a planar aligned texture at 33.0 °C (white or black arrows indicate polarizer and analyzer position, red arrow shows rubbing direction of the cell).

Au3 in **LC1** is as follows. We first preload approximately 10% (v/v) of the total amount of the **Au3** NP in *n*-hexane solution (total of 0.5 mL) in the LC test cell and use the remaining 90% (v/v) of this NP solution to prepare the LC/NP suspension in the same way as described for the first set of experiments. Thereafter, the cell was carefully heated to evaporate the solvent overnight (at a temperature slightly above the bp of *n*-hexane, ~ 70 °C) to ensure complete removal of all solvent before filling the planar test cell with the LC/NP suspension.

Figure 5a shows the more or less homogeneous vertical alignment (very few birefringent stripe domains) of the cell prepared by this NP preloading process, and instead of thermal alignment switch, only vertical alignment was observed over the entire nematic phase range of **LC1**. As observed in previous studies, the part of Au NPs immobilized at the interface during the preloading can again be redispersed in the LC bulk by heating the cell above $T_{Iso\text{-}N}$, followed by cooling back to the N phase while applying a dc electric field above the threshold voltage ($V > V_{th}$) for this mixture (dual alignment and electro-optic mode (93), Figure 5b). Both stable modes can be independently prepared simply by choosing to apply an electric field on cooling below $T_{Iso\text{-}N}$ or not. The same effect for preloading the cell with a small amount of the Au NPs was also observed for other LC/NP combinations such as 5 wt % and 10 wt % of **Au1** - **Au3** in **LC1** and **LC2** (see, for example **LC2** doped with 5 wt % **Au2** shown in Figures 5c and 5d).

To demonstrate that a process, similar to the preloading described above, that would homogeneously distribute the Au NPs over a glass or ITO-coated glass surface could also be designed to be more manufacturing-friendly, we also attempted the use of spin-coating of **Au1** NPs dispersed in **LC1** on untreated glass slides. After evaporation of the solvent (ethyl acetate), the thin film was imaged using AFM in tapping mode (Figure 6). One can see an almost even

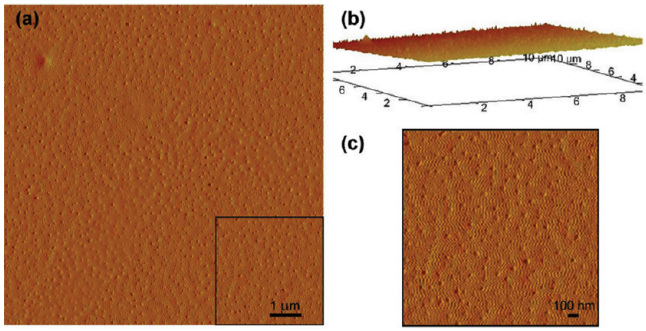

FIGURE 6. Tapping mode AFM image of a 5 wt % Au1 in LC1 suspension after spin-coating and drying: (a) amplitude, (b) 3D (height profile), and (c) magnified section of image a.

distribution of the Au NPs on the surface (Figure 6a and magnified section in 6c), which is characterized by small, almost spherical protrusions (~20−25 nm in diameter and height, see Figure 6b) that we attribute to either individual or small assemblies of Au NPs covered by the nematic LC.

Switching and Alignment between ITO-Coated Glass Slides. Using doped NPs to control the alignment of nematic LCs as outlined above is a relatively new concept, and if both components and the sample preparation are optimized to allow for stable, long-term alignment, advantages such as simplicity and easy surface modification of metal NPs could pave the way for LCDs without the need of additional alignment layers. In addition, as described in previous work, metal NPs (Au, Ag) and certain quantum dots can significantly improve other important parameters of nematic LCs such as threshold voltage, dielectric properties, and elastic constants due to the intrinsic electronic properties of metal NPs and quantum dots (93, 96, 98).

On the basis of our initial success in obtaining a thermal-history-dependent dual alignment and electro-optic switching phenomenon and alignment control using planar LC cells, we were now interested to extent these studies to cells only coated with a thin, transparent layer of ITO (no polyimide alignment layers).

Because of their importance for VA-mode LCDs, we first tested the LC alignment of a nematic **LC3** with negative dielectric anisotropic ($\Delta\epsilon < 0$). Vertical alignment of **LC3** doped with 5 wt % **Au2** was achieved by sandwiching the LC/NP suspension between two ITO-coated glass slides without spacers. Figure 7a shows the textures of **LC3** doped with 5 wt % **Au2**, and clearly shows larger areas of vertical alignment with the typically observed birefringent stripes. Upon application of a dc electric field (5 V), **LC3** switches to a planar, birefringent state, as expected for a nematic LC with $\Delta\epsilon < 0$ (Figure 7b). Also, the quality of this planar alignment is reasonably good given that no planar alignment layers are present.

To show that similar result can also be obtained with an LC with positive dielectric anisotropic ($\Delta\epsilon > 0$), we also prepared a cell with **LC1** doped with 5 wt % **Au1**. The suspension of **LC1** doped with **Au1** was first filled into an ITO-coated cell with a cell gap of ~12 μm using Mylar spacers. This time, vertical alignment is achieved in most areas of this thin film, but the quality of the vertical alignment is somewhat compromised, likely caused by the formation of NP aggregates; "leaking" of light can be observed in some areas (Figure 7c). After applying a 5 V dc electric field, a *Schlieren*-like texture was observed (Figure 7d), which means the LC molecules in these domains are reoriented planar to the surface, or at least with a significantly lower tilt. This type of switching of a nematic LC with $\Delta\epsilon > 0$ is most likely related to the fact that the Au NPs residing at the interface (the portion not dispersed in the bulk) act as local capacitors, as previously discussed in more detail (93).

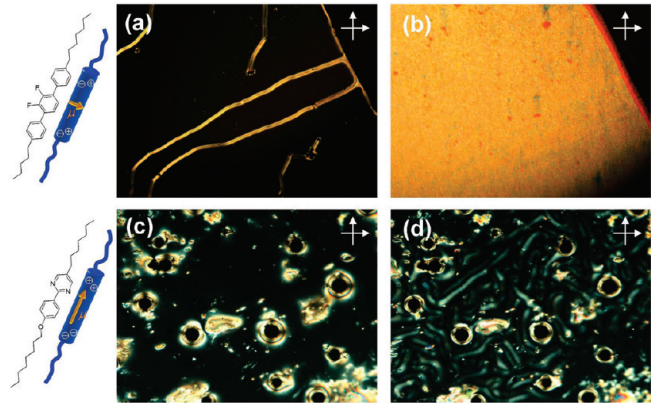

FIGURE 7. POM photomicrographs of: (a) thin film of LC3 doped with 5 wt % Au2 at 71.0 °C, (b) same area while applying a 5 V dc electric field, (c) 12 μm thick film of LC1 doped with 5 wt % Au1 at 62.0 °C, (d) same area while applying a 5 V dc electric field (white or black arrows indicate polarizer and analyzer position).

To highlight the role of the Mylar spacers in these experiments, some additional comments are necessary. In fact, it is easy to achieve complete homeotropic alignment for all LCs, **LC1**−**LC3** in thin films (<5 μm) via doping with **Au1** and **Au2**. However, we have only been able to obtain reasonable alignment quality in thicker films for **LC1** (least polar, no polar functional groups, heteroaromatic). This shows that even structural changes in the nematic LC can have an impact on the alignment quality in these systems. It seems that in the absence of alignment layers (as for the ITO-coated glass slides used here), confinement of these films in very thin layers helps to obtain homeotropic alignment. As soon as the film thickness increases to more than 5 to 6 μm, bulk effects become dominant, and the alignment in the field-OFF state, as well as the textures observed in the field-ON state, become much less defined.

However, particularly the alignment and switching of **LC3** with $\Delta\epsilon < 0$ will have great potential applications for VA-mode LC displays by providing several advantages such as no need for alignment layers and improved electro-optic characteristics as a result of metal NP doping. In addition, as shown in Figure 5 above, using preloading and planar alignment layers, both types of LCs, with $\Delta\epsilon < 0$ and with $\Delta\epsilon > 0$, could be used for VA-mode displays.

CONCLUSION

We have shown that the alignment of nematic LCs can be tuned, reversed and manipulated by doping them with alkyl thiolate-capped Au NPs. The temperature- and concen-

tration-dependent, and in some cases rather sudden change of the LC alignment is governed by the different solubility of the Au NPs initially in the isotropic phase, but also in the nematic phase itself. Hence, the alignment of the NP-doped nematics significantly depends on the order parameter (i.e., on the temperature) and ordering either in the bulk or around the NPs residing at the interface, the concentration, and on the sample preparation conditions. In principle, all phenomena discussed here reflect the level of "incompatibility" of certain Au NPs in nematic LC hosts. Ideally, functionalized Au NPs require a minimum solubility in the LC host to prevent aggregation, yet a certain incompatibility (depending on the above-mentioned parameters) is critical to induce the described alignment effects. It is not clear, for example, if decorating metal NPs with nematic molecules as detailed by Mehl et al. (114) would improve the usefulness of NPs as alignment materials for LCDs. Recent experiments in our lab showed that conventional miscibility rules between LC hosts and organic dopants do not strictly apply to NP-doped nematic mixtures (96).

The results described here also provide experimental confirmation of some molecular dynamics simulations recently described by Smith and Glaser (111) showing how anchoring conditions (planar vs homeotropic anchoring) affect solubility and NP aggregation depending on the NP concentration and temperature (Iso vs N, and within the N phase). In our work, this NP aggregation manifests itself by the segregation of the NPs on the LC-alignment layer (glass or ITO) interfaces producing temperature- and concentration-dependent alignment effects. We conclude that tuning structure−property relationships between nematic LCs (or nematic LC mixtures) and functionalized metal or semiconductor NPs, combined with approaches to unequivocally proof of location and distribution of the Au NPs in the LC host (currently ongoing in our laboratory), will provide a better understanding of these LC/NP systems. In addition, the lessons learned form these experiments could also prove to be very important for NP-assisted improvements of LC display application. In due course, doping NPs in nematics to control the orientation of the LCs could open up new possibilities for alignment layer free LC displays with the added beneficial contributions of the intrinsic electronic properties of the NP dopants.

Acknowledgment. This work was financially supported by the Natural Sciences and Engineering Research Council (NSERC) of Canada, by the Canada Foundation for Innovation (CFI), the Manitoba Research and Innovation Fund (MRIF), and the University of Manitoba (via IPM Demonstration Project Grants). The authors would also like to extend thanks to Prof. M. Chaturvedi for access to TEM, as well as Prof. D. Thomson for access to AFM and D. Chrusch for help with AFM.

Supporting Information Available: A movie clip of the thermal alignment switch of **LC1** doped with 2 wt % **Au1** and more information regarding the preloading of the test cells. This material is available free of charge via the Internet at http://pubs.acs.org.

REFERENCES AND NOTES

(1) Hong, H. K.; Lim, M. *Liq. Cryst.* **2009**, *36*, 109–113.
(2) Vrecko, A.; Pirs, J.; Bazec, M.; Ponikvar, D. *Appl. Opt.* **2008**, *47*, 2623–2629.
(3) Ren, H. W.; Lin, Y. H.; Fan, Y. H.; Wu, S. T. *J. Appl. Phys.* **2004**, *96*, 3609–3611.
(4) Huang, C. Y.; Fu, K. Y.; Lo, K. Y.; Tsai, M. S. *Optics Express* **2003**, *11*, 560–565.
(5) Brake, J. M.; Daschner, M. K.; Luk, Y. Y.; Abbott, N. L. *Science* **2003**, *302*, 2094–2097.
(6) Price, A. D.; Schwartz, D. K. *J. Am. Chem. Soc.* **2008**, *130*, 8188–8194.
(7) Cadwell, K. D.; Lockwood, N. A.; Nellis, B. A.; Alf, M. E.; Willis, C. R.; Abbott, N. L. *Sensor Actuat. B, Chem.* **2007**, *128*, 91–98.
(8) Govindaraju, T.; Bertics, P. J.; Raines, R. T.; Abbott, N. L. *J. Am. Chem. Soc.* **2007**, *129*, 11223–11231.
(9) Brake, J. M.; Abbott, N. L. *Langmuir* **2007**, *23*, 8497–8507.
(10) Guzman, O.; Abbott, N. L.; de Pablo, J. J. *J. Chem. Phys.* **2005**, *122*, 184711.
(11) Choi, M. C.; Kim, Y.; Ha, C. S. *Prog. Polym. Sci.* **2008**, *33*, 581–630.
(12) Ishii, Y. *J Disp. Technol.* **2007**, *3*, 351–360.
(13) Uchida, T.; Ishinabe, T. *MRS Bull.* **2002**, *27*, 876–879.
(14) Hoogboom, J.; Rasing, T.; Rowan, A. E.; Nolte, R. J. M. *J. Mater. Chem.* **2006**, *16*, 1305–1314.
(15) van Haaren, J. *Nature* **2001**, *411*, 29–30.
(16) Guo, M. C.; Wang, X. G. *Eur. Polym. J.* **2009**, *45*, 888–898.
(17) Sarkar, A.; Halhalli, M. R.; Kulkarni, A. D.; Wadgaonkar, P. P. *J. Appl. Polym. Sci.* **2009**, *112*, 461–472.
(18) Hahm, S. G.; Lee, S. W.; Lee, T. J.; Cho, S. A.; Chae, B.; Jung, Y. M.; Bin Kim, S.; Ree, M. *J. Phys. Chem. B* **2008**, *112*, 4900–4912.
(19) Lee, S. J.; Jung, J. C.; Lee, S. W.; Ree, M. *J. Polym. Sci. Pol. Chem.* **2004**, *42*, 3130–3142.
(20) Lai, H.; Liu, X. Y.; Qin, L.; Li, M.; Gu, Y. *Liq. Cryst.* **2009**, *36*, 173–178.
(21) Lee, S. K.; Oh, B. Y.; Kim, Y. H.; Ok, C. H.; Kim, B. Y.; Hwang, J. Y.; Seo, D. S. *Jpn. J. Appl. Phys.* **2009**, *48*, 011502.
(22) Liu, Z. J.; Yu, F. F.; Zhang, Q.; Zeng, Y.; Wang, Y. G. *Eur. Polym. J.* **2008**, *44*, 2718–2727.
(23) Usami, K.; Sakamoto, K.; Yokota, J.; Uehara, Y.; Ushioda, S. *Thin Solid Films* **2008**, *516*, 2652–2655.
(24) Lee, J. H.; Kang, D.; Clarke, C. M.; Rosenblatt, C. *J. Appl. Phys.* **2009**, *105*, 023508.
(25) Jeng, S. C.; Hwang, S. J.; Yang, C. Y. *Opt. Lett.* **2009**, *34*, 455–457.
(26) Lee, Y. J.; Gwag, J. S.; Kim, Y. K.; Jo, S. I.; Kang, S. G.; Park, Y. R.; Kim, J. H. *Appl. Phys. Lett.* **2009**, *94*, 041113.
(27) Wu, W. Y.; Wang, C. C.; Fuh, A. Y. G. *Opt. Express* **2008**, *16*, 17131–17137.
(28) Yi, Y.; Farrow, M. J.; Korblova, E.; Walba, D. M.; Furtak, T. E. *Langmuir* **2009**, *25*, 997–1003.
(29) Droge, S.; O'Neill, M.; Lobbert, A.; Kitney, S. P.; Kelly, S. M.; Wei, P.; Dong, D. W. *J. Mater. Chem.* **2009**, *19*, 274–279.
(30) Chigrinov, V. G.; Kwok, H. S.; Hasebe, H.; Takatsu, H.; Takada, H. *J. Soc. Inf. Display* **2008**, *16*, 897–904.
(31) Sava, I. *Mater. Plast.* **2008**, *45*, 404–408.
(32) Usami, K.; Sakamoto, K.; Yokota, J.; Uehara, Y.; Ushioda, S. *J. Appl. Phys.* **2008**, *104*, 113528.
(33) Osterman, J.; Tong, A. P.; Skarp, K.; Chigrinov, V.; Kwok, H. S. *J. Soc. Inf. Display* **2005**, *13*, 1003–1009.
(34) Kiselev, A. D.; Chigrinov, V.; Huang, D. D. *Phys. Rev. E* **2005**, *72*, 061703.
(35) Huang, D. D.; Pozhidaev, E. P.; Chigrinov, V. G.; Cheung, H. L.; Ho, Y. L.; Kwok, H. S. *Displays* **2004**, *25*, 21–29.
(36) Sakamoto, K.; Usami, K.; Sasaki, T.; Ushioda, S. *Ieice T. Electron.* **2004**, *E87C*, 1936–1942.
(37) Zhao, Y. *Pure Appl. Chem.* **2004**, *76*, 1499–1508.
(38) Sakamoto, K.; Usami, K.; Sasaki, T.; Kanayama, T.; Ushioda, S. *Thin Solid Films* **2004**, *464−65*, 416–419.
(39) Lu, F. Z.; Peng, Z. H.; Zhang, L. L.; Yao, L. S.; Liu, Y.; Xuan, L. *Acta Phys., Chim. Sin.* **2009**, *25*, 273–277.
(40) Lv, F.; Peng, Z. H.; Zhang, L. L.; Yao, L. S.; Liu, Y.; Xuan, L. *Liq. Cryst.* **2009**, *36*, 43–51.
(41) Zhang, L. L.; Peng, Z. H.; Yao, L. S.; Lv, F. Z.; Xuan, L. *Liq. Cryst.* **2008**, *35*, 163–171.

(42) Lee, J. H.; Kawatsuki, N. *Mol. Cryst. Liq. Cryst.* **2007**, *470*, 19–29.
(43) Xia, Q. L.; Yu, H. F.; Lian, Y. Q.; Wang, X. G. *Acta Polym. Sin.* **2005**, 914–918.
(44) Chae, B.; Lee, S. W.; Ree, M.; Kim, S. B. *Vib. Spectrosc.* **2002**, *29*, 69–72.
(45) Yaroshchuk, O.; Sergan, T.; Kelly, J.; Gerus, I. *Jpn. J. Appl. Phys. Part 1* **2002**, *41*, 275–279.
(46) Choi, J.; Lim, J.; Song, K. G. *Polymer (Korea)* **2006**, *30*, 417–421.
(47) Wirnsberger, G.; Scott, B. J.; Chmelka, B. F.; Stucky, G. D. *Adv. Mater.* **2000**, *12*, 1450–1454.
(48) Galvin, J. M.; Schuster, G. B. *Supramol. Sci.* **1998**, *5*, 89–100.
(49) Ichimura, K.; Hayashi, Y.; Goto, K.; Ishizuki, N. *Thin Solid Films* **1993**, *235*, 101–107.
(50) Ichimura, K.; Hayashi, Y.; Ishizuki, N. *Chem. Lett.* **1992**, 1063–1066.
(51) Kellar, E. J. C.; Williams, G.; Krongauz, V.; Yitzchaik, S. *J. Mater. Chem.* **1991**, *1*, 331–337.
(52) Kang, H.; Kang, D.; Lee, J. C. *Liq. Cryst.* **2008**, *35*, 1005–1013.
(53) Hah, H.; Sung, S. J.; Cho, K. Y.; Park, J. K. *Polym. Bull.* **2008**, *61*, 383–390.
(54) Vretik, L. O.; Syromyatnikov, V. G.; Zagniy, V. V.; Savchuk, E. A.; Yaroshchuk, O. V. *Mol. Cryst. Liq. Cryst.* **2008**, *486*, 1099–1107.
(55) Kim, C.; Wallace, J. U.; Chen, S. H.; Merkel, P. B. *Macromolecules* **2008**, *41*, 3075–3080.
(56) Kang, H.; Park, J. S.; Kang, D.; Lee, J. C. *Macromol. Chem. Phys.* **2008**, *209*, 1900–1908.
(57) Hoogboom, J.; Elemans, J. A. A. W.; Rowan, A. E.; Rasing, T. H. M.; Nolte, R. J. M. *Phil. Trans. R. Soc., Math. Phys. Eng. Sci.* **2007**, *365*, 1553–1576.
(58) Hoogboom, J.; Elemans, J. A. A. W.; Rasing, T.; Rowan, A. E.; Nolte, R. J. M. *Polym. Int.* **2007**, *56*, 1186–1191.
(59) Hoogboom, J.; Garcia, P. M. L.; Otten, M. B. J.; Elemans, J. A. A. W.; Sly, J.; Lazarenko, S. V.; Rasing, T.; Rowan, A. E.; Nolte, R. J. M. *J. Am. Chem. Soc.* **2005**, *127*, 11047–11052.
(60) Hoogboom, J.; Behdani, M.; Elemans, J. A. A. W.; Devillers, M. A. C.; de Gelder, R.; Rowan, A. E.; Rasing, T.; Nolte, R. M. *Angew. Chem., Int. Ed.* **2003**, *42*, 1812–1815.
(61) Koenig, G. M.; Meli, M. V.; Park, J. S.; de Pablo, J. J.; Abbott, N. L. *Chem. Mater.* **2007**, *19*, 1053–1061.
(62) Shah, R. R.; Heinrichs, D. M.; Abbott, N. L. *Colloids Surf., A* **2000**, *174*, 197–208.
(63) Gupta, V. K.; Miller, W. J.; Pike, C. L.; Abbott, N. L. *Chem. Mater.* **1996**, *8*, 1366–1369.
(64) Drawhorn, R. A.; Abbott, N. L. *J. Phys. Chem.* **1995**, *99*, 16511–16515.
(65) Wilderbeek, H. T. A.; Teunissen, J. P.; Bastiaansen, C. W. M.; Broer, D. J. *Adv. Mater.* **2003**, *15*, 985–988.
(66) Wilderbeek, H. T. A.; van der Meer, F. J. A.; Feldman, K.; Broer, D. J.; Bastiaansen, C. W. M. *Adv. Mater.* **2002**, *14*, 655–658.
(67) Harris, K. D.; van Popta, A. C.; Sit, J. C.; Broer, D. J.; Brett, M. J. *Adv. Funct. Mater.* **2008**, *18*, 2147–2153.
(68) Wakefield, N. G.; Elias, A. L.; Brett, M. J.; Sit, J. C.; Broer, D. J. *Mol. Cryst. Liq. Cryst.* **2007**, *475*, 85–96.
(69) Oh, B. Y.; Lee, W. K.; Kim, Y. H.; Seo, D. S. *J. Appl. Phys.* **2009**, *105*, 054506.
(70) Park, H. G.; Oh, B. Y.; Kim, Y. H.; Kim, B. Y.; Han, J. M.; Hwang, J. Y.; Seo, D. S. *Electrochem. Solid State* **2009**, *12*, J37−J39.
(71) Park, H. G.; Kim, Y. H.; Oh, B. Y.; Lee, W. K.; Kim, B. Y.; Seo, D. S.; Hwang, J. Y. *Appl. Phys. Lett.* **2008**, *93*, 233507.
(72) Son, P. K.; Jo, B. K.; Kim, J. C.; Yoon, T. H.; Rho, S. J.; Shin, S. T.; Kim, J. S.; Lim, S. K.; Souk, J. H. *Jpn. J. Appl. Phys.* **2008**, *47*, 8476–8478.
(73) Kim, Y. H.; Park, H. G.; Oh, B. Y.; Kim, B. Y.; Paek, K. K.; Seo, D. S. *J. Electrochem. Soc.* **2008**, *155*, J371−J374.
(74) Oh, B. Y.; Lee, K. M.; Kim, B. Y.; Kim, Y. H.; Han, J. W.; Han, J. M.; Lee, S. K.; Seo, D. S. *J. Appl. Phys.* **2008**, *104*, 064502.
(75) Oh, B. Y.; Lim, J. H.; Lee, K. M.; Kim, Y. H.; Kim, B. Y.; Han, J. M.; Lee, S. K.; Seo, D. S.; Hwang, J. Y. *Electrochem. Solid State* **2008**, *11*, H331−H334.
(76) Scharf, T. F.; Shlayen, A.; Gernez, C.; Basturk, N.; Grupp, J. *Mol. Cryst. Liq. Cryst.* **2004**, *412*, 1745–1755.
(77) Song, K. M.; Rho, S. J.; Ahn, H. J.; Kim, K. C.; Baik, H. K.; Hwang, J. Y.; Jo, Y. M.; Seo, D. S.; Lee, S. J. *Jpn. J. Appl. Phys.* **2004**, *43*, 1577–1580.
(78) Chaudhari, P.; Lacey, J.; Doyle, J.; Galligan, E.; Lien, S. C. A.; Callegari, A.; Hougham, G.; Lang, N. D.; Andry, P. S.; John, R.; Yang, K. H.; Lu, M. H.; Cai, C.; Speidell, J.; Purushothaman, S.; Ritsko, J.; Samant, M.; Stohr, J.; Nakagawa, Y.; Katoh, Y.; Saitoh, Y.; Sakai, K.; Satoh, H.; Odahara, S.; Nakano, H.; Nakagaki, J.; Shiota, Y. *Nature* **2001**, *411*, 56–59.
(79) Hegde, G.; Yaroshchuk, O.; Kravchuk, R.; Murauski, A.; Chigrinov, V.; Kwok, H. S. *J. Soc. Inf. Display* **2008**, *16*, 1075–1079.
(80) Yaroshchuk, O.; Parri, O.; Kravchuk, R.; Satayesh, S.; Reijme, M. *J. Soc. Inf. Display* **2008**, *16*, 905–909.
(81) Wu, K. Y.; Hwang, J.; Lee, C. Y.; Tang, H. C.; Liu, Y. L.; Liu, C. H.; Wei, H. K.; Kou, C. S. *Thin Solid Films* **2008**, *517*, 905–908.
(82) Chen, T. H.; Liu, C. H.; Teng, J. T.; Lee, C. Y.; Lin, S. *Jpn. J. Appl. Phys.* **2008**, *47*, 6437–6441.
(83) Shah, H. J.; Delaine, D.; Fontecchio, A. K. *J. Display Technol.* **2008**, *4*, 160–165.
(84) Yaroshchuk, O. V.; Kiselev, A. D.; Kravchuk, R. M. *Phys. Rev. E* **2008**, *77*, 031706.
(85) Choi, S. H.; Oh, B. Y.; Kim, B. Y.; Han, J. M.; Han, J. W.; Ok, C. H.; Lee, S. K.; Hwang, J. Y.; Seo, D. S. *Mol. Cryst. Liq. Cryst.* **2008**, *480*, 3–9.
(86) Lee, C. Y.; Liu, C. H.; Chen, C. W.; Miki, S.; Chen, H. M. P.; Lin, S.; Su, P. H.; Lee, C. D. *J. Soc. Inf. Display* **2008**, *16*, 71–75.
(87) Hong, H.; Shin, H.; Chung, I. *J. Display Technol.* **2007**, *3*, 361–370.
(88) Doyle, J. P.; Chaudhari, P.; Lacey, J. L.; Galligan, E. A.; Lien, S. C.; Callegari, A. C.; Lang, N. D.; Lu, M.; Nakagawa, Y.; Nakano, H.; Okazaki, N.; Odahara, S.; Katoh, Y.; Saitoh, Y.; Sakai, K.; Satoh, H.; Shiota, Y. *Nucl. Instrum. Meth. B* **2003**, *206*, 467–471.
(89) Hwang, S. J.; Jeng, S. C.; Yang, C. Y.; Kuo, C. W.; Liao, C. C. *J. Phys. D, Appl. Phys* **2009**, *42*, 025102.
(90) Teng, W. Y.; Jeng, S. C.; Kuo, C. W.; Lin, Y. R.; Liao, C. C.; Chin, W. K. *Opt. Lett.* **2008**, *33*, 1663–1665.
(91) Qi, H.; Hegmann, T. *J. Mater. Chem.* **2008**, *18*, 3288–3294.
(92) Kundu, S.; Akimoto, M.; Hirayama, I.; Inoue, M.; Kobayashi, S.; Takatoh, K. *Jpn. J. Appl. Phys.* **2008**, *47*, 4751–4754.
(93) Qi, H.; Kinkead, B.; Hegmann, T. *Adv. Funct. Mater.* **2008**, *18*, 212–221.
(94) Kuo, C. W.; Jeng, S. C.; Wang, H. L.; Liao, C. C. *Appl. Phys. Lett.* **2007**, *91*, 141103.
(95) Qi, H.; Hegmann, T. *J. Mater. Chem.* **2006**, *16*, 4197–4205.
(96) Qi, H.; Kinkead, B.; Marx, V. M.; Zhang, H. R.; Hegmann, T. *ChemPhysChem* **2009**, *10*, 1211–1218.
(97) Qi, H.; O'Neil, J.; Hegmann, T. *J. Mater. Chem.* **2008**, *18*, 374–380.
(98) Qi, H.; Kinkead, B.; Hegmann, T. *Proc. SPIE* **2008**, *6911*, 691106.
(99) Dhar, R.; Pandey, A. S.; Pandey, M. B.; Kumar, S.; Dabrowsi, R. *Appl. Phys. Express* **2008**, *1*, 121501.
(100) Lu, S. Y.; Chien, L. C. *Opt. Express* **2008**, *16*, 12777–12785.
(101) Mrozek, R. A.; Kim, B. S.; Holmberg, V. C.; Taton, T. A. *Nano Lett* **2003**, *3*, 1665–1669.
(102) Talarico, M.; Carbone, G.; Barberi, R.; Golemme, A. *Appl. Phys. Lett.* **2004**, *85*, 528–530.
(103) Goodby, J. W.; Saez, I. M.; Cowling, S. J.; Gortz, V.; Draper, M.; Hall, A. W.; Sia, S.; Cosquer, G.; Lee, S. E.; Raynes, E. P. *Angew. Chem., Int. Ed.* **2008**, *47*, 2754–2787.
(104) Hegmann, T.; Qi, H.; Marx, V. M. *J. Inorg. Organomet. Polym. Mater.* **2007**, *17*, 483–508.
(105) Giljohann, D. A.; Seferos, D. S.; Patel, P. C.; Millstone, J. E.; Rosi, N. L.; Mirkin, C. A. *Nano Lett* **2007**, *7*, 3818–3821.
(106) Huang, W. Y.; Qian, W.; Jain, P. K.; El-Sayed, M. A. *Nano Lett* **2007**, *7*, 3227–3234.
(107) Prasad, S. K.; Sandhya, K. L.; Nair, G. G.; Hiremath, U. S.; Yelamaggad, C. V.; Sampath, S. *Liq. Cryst.* **2006**, *33*, 1121–1125.
(108) Qi, H.; Hegmann, T. *J. Am. Chem. Soc.* **2008**, *130*, 14201–14206.
(109) Da Cruz, C.; Sandre, O.; Cabuil, V. *J. Phys. Chem. B* **2005**, *109*, 14292–14299.
(110) Bezrodna, T.; Chashechnikova, I.; Gavrilko, T.; Puchkovska, G.; Shaydyuk, Y.; Tolochko, A.; Baran, J.; Drozd, M. *Liq. Cryst.* **2008**, *35*, 265–274.
(111) Xu, J. Q.; Bedrov, D.; Smith, G. D.; Glaser, M. A. *Phys. Rev. E* **2009**, *79*, 011704.
(112) De, M.; Ghosh, P. S.; Rotello, V. M. *Adv. Mater.* **2008**, *20*, 4225–4241.
(113) Ghosh, P.; Han, G.; De, M.; Kim, C. K.; Rotello, V. M. *Adv. Drug Delivery Rev.* **2008**, *60*, 1307–1315.
(114) Zeng, X. P.; Liu, F.; Fowler, A. G.; Ungar, G.; Cseh, L.; Mehl, G. H.; Macdonald, J. E. *Adv. Mater.* **2009**, *21*, 1746–1750, and references therein.

AM9002815